Carbohydrate Coating Reduces Adhesion of Biofilm-Forming *Bacillus subtilis* to Gold Surfaces

S. Kesel,[a] A. Mader,[a] P. H. Seeberger,[b,c] O. Lieleg,[d] M. Opitz[a]

Center for NanoScience, Faculty of Physics, Ludwig-Maximilians-Universität München, Munich, Germany[a]; Max Planck Institute of Colloids and Interfaces, Department of Biomolecular Systems, Berlin, Germany[b]; Freie Universität Berlin, Institute for Chemistry and Biochemistry, Berlin, Germany[c]; Institute for Medical Engineering IMETUM and Department for Medical Engineering, Technische Universität München, Garching, Germany[d]

The growth of bacterial biofilms in pipes and food tanks causes severe problems in industry. Biofilms growing on medical implants or catheters are of great concern, as they can cause serious infections and decrease the functionality of the medical device. The prevention of bacterial adhesion—the first step in colonization and biofilm formation—is therefore very important. Current research comprises alterations in surface properties, the prevention of adhesin biosynthesis, inhibition with receptor analogs, or the development of anti-adhesive vaccines. We present a new approach that allows us to study bacterial adhesion with high sensitivity in real-time while testing several different surfaces in parallel. Using the cantilever-array technique we demonstrate that coating of gold surfaces with mono- or disaccharides results in a reduction of the bacterial adhesion of the biofilm-forming bacterium *Bacillus subtilis* NCIB 3610 to these gold surfaces. This reduction in bacterial adhesion is independent of the studied carbohydrate. Using several mutant strains, we investigate the underlying molecular interactions, and our results suggest that adhesion to gold surfaces is mediated by thiol groups present in proteins of the bacterial cell membrane or biofilm matrix proteins expressed at low levels by the wild-type strain. Furthermore, our data indicate that the adhesion of *B. subtilis* NCIB 3610 to carbohydrate-coated gold surfaces is facilitated by interactions between carbohydrates installed on the cantilever gold surface and an exopolysaccharide expressed by this strain. Understanding general and specific contributions of molecular interactions mediating bacterial adhesion will enable its prevention in the future.

The term "biofilm" describes a community of microorganisms that adhere to a surface. Biofilm architecture is provided by a self-produced matrix of extracellular polymeric substances (EPSs), a mix of polysaccharides, proteins, lipids, and nucleic acid (1). The EPS secreted by the microbial cells makes up to 50 to 90% of the total organic material in biofilms (2, 3) and provides increased resistance to antibiotics and environmental stresses. Biofilms can grow on various surfaces and in many different environments, a phenomenon that constitutes major problems in industry and medicine (2). Biofouling can lead to material degradation (biocorrosion) (4), and biofilms on surfaces in food production enhance the risk for product contamination with pathogens (5). Biofilm-associated bacteria on medical implants or catheters are of great concern because they can cause serious infections and decrease the functionality of the medical device (2). Therefore, the prevention of bacterial adhesion (6–9) is of great importance since bacterial adhesion to surfaces is the first step in colonization, invasion, and biofilm formation (10). One of the best-studied biofilm-forming organisms is *Bacillus subtilis* NCIB 3610. Its matrix is composed of an exopolysaccharide produced by the *epsA-O* operon (11) and an amyloid fiber-forming protein, TasA (12). A second biofilm matrix protein, BslA is a self-assembling hydrophobin on the surface of the *B. subtilis* biofilm (13, 14). Recent studies on biofilm formation focus on biofilm growth on solid surfaces or in microfluidic devices (15–20). However, most of these studies neglect the initial phase of biofilm formation, namely, the initial attachment or bacterial adhesion to surfaces. Here, we present a new approach: using a cantilever-based biosensor, we studied the attachment of biofilm-forming bacteria to surfaces. Cantilever-based biosensors have been used to study DNA or protein interactions (21), and it has been shown that carbohydrate-protein interactions can be detected with picomolar sensi-

tivity (22). In former studies, we and other groups verified the suitability of glycan-cantilever array sensors for the detection and discrimination of different *Escherichia coli* strains with distinct mannoside binding properties (23, 24), and the suitability of these devices for analysis of filamentous fungi growth was demonstrated (25). The high sensitivity of this approach allows for the detection of single bacteria binding to the cantilever surface. Due to changes in surface stress induced upon bacterial adhesion, cantilever bending can be detected by the deflection of a laser beam. Furthermore, substances secreted by the bacteria alter the surface stress and with it the deflection signal. Thereby, we can study adhesion of *B. subtilis* NCIB 3610 to single cantilevers and investigate the role of basal EPS expression and secretion for the attachment of this biofilm-forming *B. subtilis*.

One means to prevent bacterial adhesion constitutes coating of different surfaces with glycans or complex glycoproteins (6, 9). However, if and to what degree sugar motifs vary in their efficiency to reduce bacterial adhesion on hard surfaces remains poorly understood. Here, we present a detailed study on the adhesion of *B. subtilis* NCIB 3610 to gold cantilevers. We demonstrate that coating of these cantilevers with different mono- and
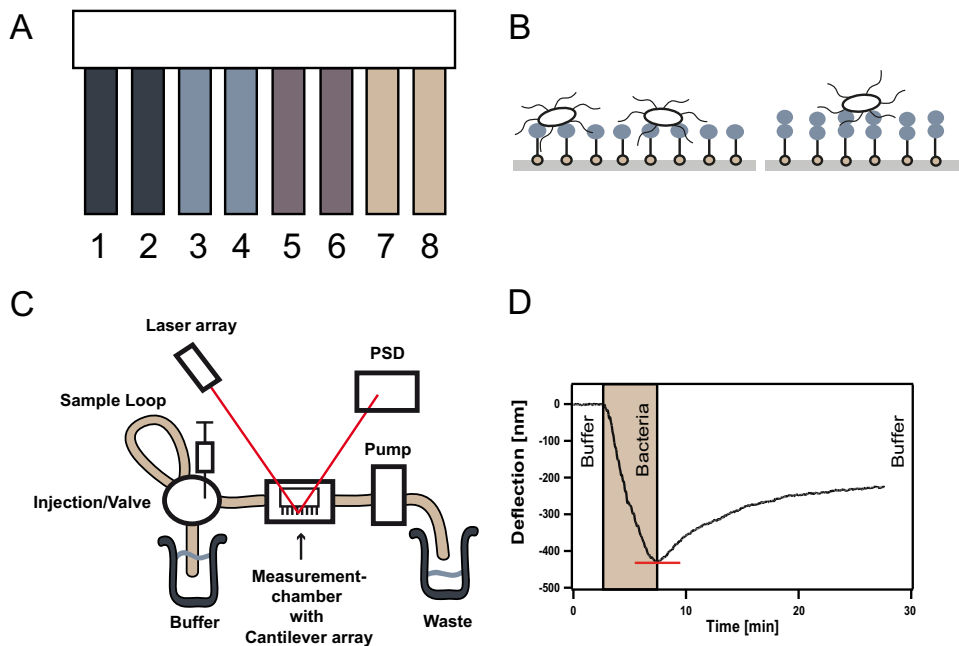
FIG 1 Display of method. (A) Functionalization of the eight single cantilevers of a cantilever array: cantilevers 1 and 2 with galactose, cantilevers 3 and 4 with mannose, cantilevers 5 and 6 with lactose, and cantilevers 7 and 8 unfunctionalized gold cantilever. (B) Assembly of the monosaccharides (left) and disaccharides (right), depicted by blue balls, on the gold cantilever surface via their installed thiols (light brown balls). Single bacteria can then adhere to the carbohydrate-coated gold surface. Note that neither the carbohydrates nor the bacteria are drawn to scale. One bacterial cell is able to establish contact with multiple carbohydrates. (C) Schematic of the experimental setup. Bacteria are added to the running buffer via a Hamilton syringe. At a constant flow rate, bacteria then pass by the cantilever array installed in the measurement chamber. Bacterial attachment to the eight single cantilevers leads to cantilever bending that in turn is detected by a change in laser deflection at the PSD (position sensitive detector). Each cantilever is analyzed with a separate laser; for better visibility, only one laser beam was drawn. (D) Sample measurement graph. During the first 3 min, the cantilevers are calibrated with buffer. The bacterial sample is then injected and needs about 4 min to pass the measurement chamber. The phase of bacteria passing the cantilever array is highlighted in light brown. After the bacterial sample has completely passed the cantilever array, the cantilever is flushed again with buffer. The absolute value of the minimum of the curve, called the maximal deflection, corresponds to the maximum amount of bacteria being attached to the surface and is depicted by the red line.

disaccharides reduces the adhesion efficiency of *B. subtilis* NCIB 3610, independent of the studied carbohydrate. Furthermore, we analyze the molecular interaction of the adhesion process in detail, using several mutant strains lacking the ability to produce distinct biofilm matrix components. Our data indicate that adhesion of *B. subtilis* NCIB 3610 to carbohydrate-coated surfaces is facilitated by the exopolysaccharide produced by the *epsA-O* operon.

MATERIALS AND METHODS

Cantilever functionalization. The gold-coated cantilever arrays (Fig. 1A), with eight cantilevers (500 μm by 100 μm by 1 μm) per array, were purchased from Concentris GmbH, Switzerland. They were cleaned under UV light for 1.5 h in order to remove possible impurities and smooth the gold surface (26). This step is crucial for the following functionalization step as an irregular gold surface can lead to a decrease in cantilever

sensitivity (27). The monosaccharides used in the present study, galactose, mannose, and the disaccharide lactose, all with an terminal thiol linker (Fig. 1B), were synthesized as described elsewhere (28). The glycan samples were diluted to 40 μM in 10 mM Tris buffer (pH 7). For functionalization, the gold-coated cantilevers arrays were inserted into microcapillaries filled with the thiol-carbohydrate solution. The cantilevers were incubated for 10 min in these microcapillaries and thereby exposed to the thiol-carbohydrate solution, enabling the self-assembly of the thiol-carbohydrates on the gold surface of the single cantilevers. Please note that always two cantilevers per array were functionalized with the same carbohydrate (Fig. 1A).

Strains and growth conditions. The *B. subtilis* strains used in the present study are presented in Table 1. In preparation for these experiments, bacterial cells were grown overnight in 5 ml of LB medium (Luria/Miller; Roth), with antibiotic if needed to ensure growth of the selected

TABLE 1 *B. subtilis* strains used in this study

Strain	Description	Remaining matrix composition	Antibiotic (concn [μg/ml])	Reference
NCIB 3610	Wild type	Proteins TasA and BslA, exopolysaccharide	None	54
CA017	TasA::Kan	Protein BslA, exopolysaccharide	Kanamycin (50)	18
N24	BslA::Cam	Protein TasA, exopolysaccharide	Chloramphenicol (5)	13
ZK3660	EpsA-O::Tet	Proteins TasA and BslA	Tetracycline (12.5)	37
BD630	Wild type	Unable to form proper biofilm, including exopolysaccharide	None	45

mutant strains according to Table 1, at 37°C and with shaking at 300 rpm. The overnight cultures are diluted to an optical density at 600 nm (OD_{600}) of 0.05 and grown until the strains had clearly entered the stationary phase. The culture was then centrifuged down at a 1,900 relative centrifugal force for 5 min twice and resuspended in the running buffer (100 mM NaCl, 10 mM Tris [pH 7], 0,005% Tween 20, 1 mM $CaCl_2$). Thus, changes in the ionic strength (due to a buffer change) that might contribute to the deflection signal could be excluded. The bacterial cultures were further diluted to an OD_{600} of 0.1 for the experiments.

Measurement conditions and analysis. All measurements were performed on the Cantisens research sensor platform (Concentris GmbH) (Fig. 1C) with integrated an measurement chamber with a 5-μl volume, a sample volume of 100 μl, and an automated liquid handling system and temperature control at a stability of 0.01°C. In order to equilibrate the cantilever array, it was set in the instrument at a flow rate of 0.42 μl/s and a temperature of 22°C until the thermal drift of the deflection signal of ~0.04 nm/s was constant (29). The flow rate and temperature were then held constant for all experiments. To prevent fluctuations in the results due to fabrication variances, the arrays were tested with a heat pulse (22): cantilever arrays were exposed to a temperature change of 3°C from 22 to 25°C and back. Due to their bimetal nature, the cantilevers bend, resulting in a deflection signal. Only cantilever arrays where all eight single cantilevers showed an identical deflection signal were used. The deflection signal is read out with an array of eight parallel vertical cavity surface-emitting lasers in real time. Instrument control and data analysis were performed using LabView-based software by Concentris GmbH. For data analysis, all signal curves were corrected for their drift, and the results from identically functionalized cantilevers were averaged. The start value was set to zero for each measurement. The absolute value of the minimum of the graph, which is referred to as maximal deflection (Fig. 1D) for the remainder of this article, was read out and transferred to an Igor Pro (v4.06) spreadsheet for data analysis. For the data presented in Fig. 3, the data sets were first normalized to data obtained from the gold cantilevers and then averaged over all experiments. Three measurements were performed on three separate days for each wild-type and mutant strain in the study, representing a total of 18 experiments for each strain since two single cantilevers were functionalized with the same carbohydrate. Error bars, representing the errors of the averaged, normalized values, were calculated according to Gaussian error propagation.

RESULTS

Adhesion of *B. subtilis* to gold cantilevers is attributed to protein-Au interaction. The first step in biofilm formation is the attachment (adhesion) of single bacteria to a given surface. This crucial step represents one target to prevent bacterial adhesion and with it the subsequent infection of a patient. Here, we investigate the attachment of the well-studied biofilm-forming strain *B. subtilis* NCIB 3610 to gold surfaces. Adhesion of bacterial biofilms to metal surfaces (in pipes or food tanks) causes major problems in industry (2, 30–33), but how bacteria attach to these metal surfaces is often unknown. It was shown that several metals have the ability to interact with thiol groups (34). Thiol groups present in proteins of the bacterial cell membrane could therefore mediate the initial attachment of bacteria to these metal surfaces. We chose gold-coated cantilevers as a model system to study the initial attachment of bacteria. Since gold was reported to have a very high affinity to thiol groups (34, 35), we assumed to get high deflection signals due to strong bacterial adhesion using this surface. To detect adhesion of single bacteria to gold surfaces we chose the cantilever array technique (see Materials and Methods), since adhesion to several different surfaces can be quantitatively observed in real-time in parallel with high sensitivity (22, 24). In Fig. 1C and D, a schematic of the experimental setup and a typical detection

curve is given; after flushing and calibrating the instrument with buffer, the bacterial sample is injected. For about 4 min bacteria are passing the cantilever array able to adhere to the single cantilevers. This induces a surface stress and causes the cantilever to bend, resulting in the observed deflection signal. The maximum deflection signal thereby corresponds to the maximum amount of bacteria being attached to the surface. Once the bacterial sample has completely passed the array, the instrument is again flushed with buffer. Since bacteria that only reversibly bind to the cantilever are thereby removed, the deflection signal decreases again to the value representing irreversible binding of bacteria (Fig. 1D).

In a first experiment, we investigated adhesion of *B. subtilis* NCIB 3610 to gold cantilevers (Fig. 2). We obtained a significant detection signal for bacterial adhesion of this strain to the gold cantilevers with 270 ± 30 nm, as was expected for the used bacterial density ($OD_{600} = 0.1$; see Materials and Methods). In a next step, we wanted to understand how this strain adheres to the gold cantilevers and what kind of molecular interactions are responsible for its adhesion. Such molecular interactions can result from proteins or carbohydrates in the bacterial cell membrane or from proteins or carbohydrates that are part of the biofilm matrix of *B. subtilis* NCIB 3610 and are expressed at low rates in the stationary growth phase (12, 36). To address this question, we investigated the binding of several mutant strains in comparison to this wild-type strain to our gold cantilevers (Fig. 2; see Table S1 in the supplemental material). While the complete biofilm matrix of NCIB 3610 consists of two proteins TasA and BslA (12–14), as well as an exopolysaccharide produced by the *epsA-O* operon (11), the mutant strains used in the present study lack one of these matrix components each (Table 1).

The first mutant strain of NCIB 3610 that we analyzed was a TasA knockout strain. TasA has been reported to be a fiber-forming protein present in the biofilm matrix of *B. subtilis* NCIB 3610 (12). We measured a maximal deflection signal for this strain attaching to gold cantilevers of 370 ± 30 nm. In a second mutant strain, the biofilm surface layer protein BslA (13, 14) was knocked out. For this strain we obtained a maximal deflection signal of 290 ± 30 nm. Although these two mutant strains were still able to produce one matrix protein and the exopolysaccharide, in the last mutant strain, the *epsA-O* operon necessary for exopolysaccharide production was knocked out (37), leaving this strain unable to produce the exopolysaccharide. Interestingly, the maximum deflection signal increased to 700 ± 90 nm for this strain. This finding indicated that binding of the NCIB 3610 wild-type and mutant strains to gold surfaces might be mediated by protein-Au interactions. This strong interaction could result from thiol groups (34) of proteins present in the bacterial cell membrane or being part of the biofilm matrix. The obtained high maximum deflection signal of the EpsA-O mutant binding to gold cantilevers furthermore suggested that exopolysaccharides, present in the wild-type and TasA and BslA knockout strains but absent in the EpsA-O mutant strain, could interfere with this strong protein-Au interaction, resulting in a decrease of the bacterial adhesion by 38%.

Carbohydrates reduce adhesion of *B. subtilis* NCIB 3610 to gold cantilevers. We have observed that a mutant strain that is unable to produce an exopolysaccharide bound significantly better to gold cantilevers compared to wild-type and mutant strains producing this exopolysaccharide (Fig. 2). This observation indicated that carbohydrates such as the exopolysaccharide being a part of the biofilm matrix of this *B. subtilis* strain could interfere
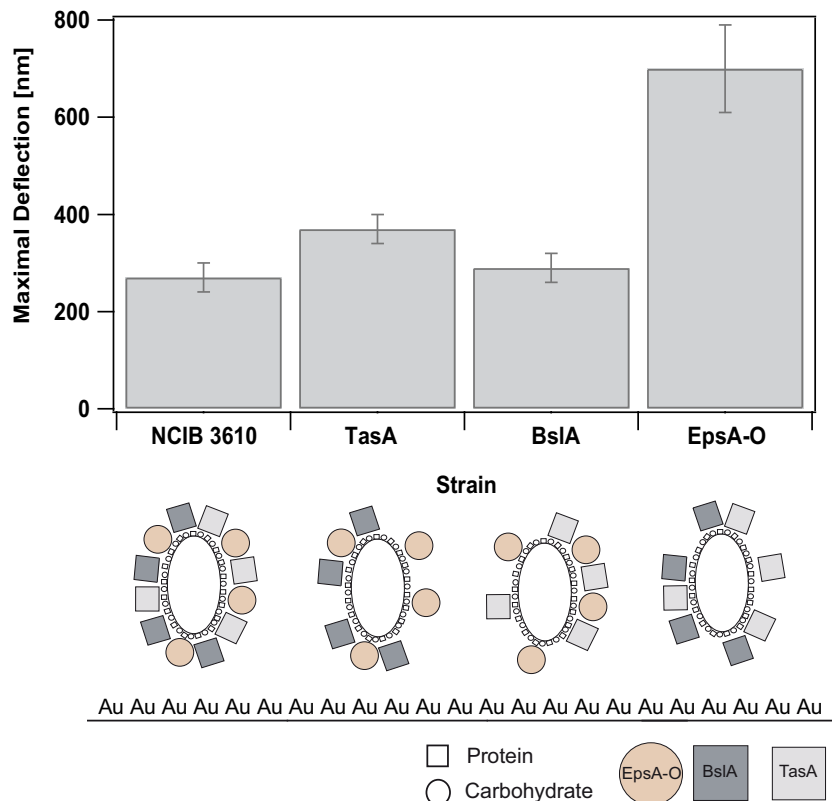
FIG 2 Comparison of the maximal deflections obtained for the different wild-type and mutant strains adhering on gold cantilevers. Maximal deflections were averaged and displayed for each strain. The error bars indicate the standard deviations. Below the bar plot, pictograms for the biofilm matrix composition for each strain are shown. Depending on the mutant strain, different interactions (protein-Au or carbohydrate-Au) with the gold cantilever (depicted with Au) are possible. Proteins are depicted as squares, and carbohydrates are depicted as circles. Note that the sizes and distributions of the carbohydrates and proteins are not drawn to scale.

with the protein-Au interaction and therefore reduce bacterial adhesion. To test this hypothesis, we additionally functionalized the pure gold cantilevers with different mono- and disaccharides. For reproducibility, two of eight single cantilevers were functionalized in the same way (Fig. 1A). Functionalization of the different carbohydrates on the gold top surface of the single cantilevers is achieved by installing a terminal thiol (28) on the carbohydrate. The carbohydrates then self-assemble on the gold top-side of the single cantilevers and can interact directly with the adhering bacteria (Fig. 1B).

We investigated adhesion of the biofilm-forming *B. subtilis* wild-type strain NCIB 3610 to these carbohydrate-coated gold cantilevers (Fig. 3; see Table S2 in the supplemental material). We chose the monocarbohydrates galactose and mannose because they represent sugars that many bacterial species can metabolize, as well as the disaccharide lactose since it represents a sugar often used in the food industry. In addition, we were also interested in addressing the question of whether bacterial adhesion differs for mono- and disaccharides. Studying the wild-type strain NCIB 3610, we found that adhesion of this strain to the carbohydrate-coated gold cantilevers was further decreased by 23% in comparison to the pure gold cantilevers (Fig. 3B), supporting our hypothesis that carbohydrates can reduce bacterial adhesion to gold surfaces. In addition, the binding efficiency was similar for the different carbohydrates tested, indicating that the reduction of bacterial adhesion to gold cantilevers can be achieved by mono-

and disaccharides in the same way. Studying our mutant strains, we obtained a similar reduction of bacterial adhesion on carbohydrate-coated cantilevers in comparison to the wild-type strain, with 16 and 15% for TasA and BslA knockout strains, respectively (Fig. 3C and D). In summary, our data support the conclusion that adhesion of *B. subtilis* NCIB 3610 to gold cantilevers is reduced by additional coating of these cantilevers with different carbohydrates.

Bacterial adhesion to carbohydrate-coated cantilevers is further reduced in a mutant strain unable to produce an exopolysaccharide. We had seen that functionalization of gold cantilevers with different mono- and disaccharides resulted in a decrease of the bacterial adhesion (Fig. 3B, C, and D). In a next step, we wanted to address the question whether a mutant strain unable to secrete an exopolysaccharide as a biofilm matrix component (37) could be further affected in its adhesion to these carbohydrate-coated gold cantilevers. Indeed, this EpsA-O knockout mutant revealed the strongest reduction in bacterial adhesion, that is, a decrease by 44% (Fig. 3E) compared to the wild-type strain (23%) (Fig. 3B) or the two mutant strains TasA and BslA (16 and 15%, respectively) (Fig. 3C and D). The reduced ability of the EpsA-O knockout mutant to bind to carbohydrate-coated gold cantilevers could be explained by the absence of carbohydrate-carbohydrate interactions (38–44) between the exopolysaccharide and the carbohydrates on the cantilever surface. To test this hypothesis, we studied a different wild-type strain, namely, BD630 (45), a deriv-
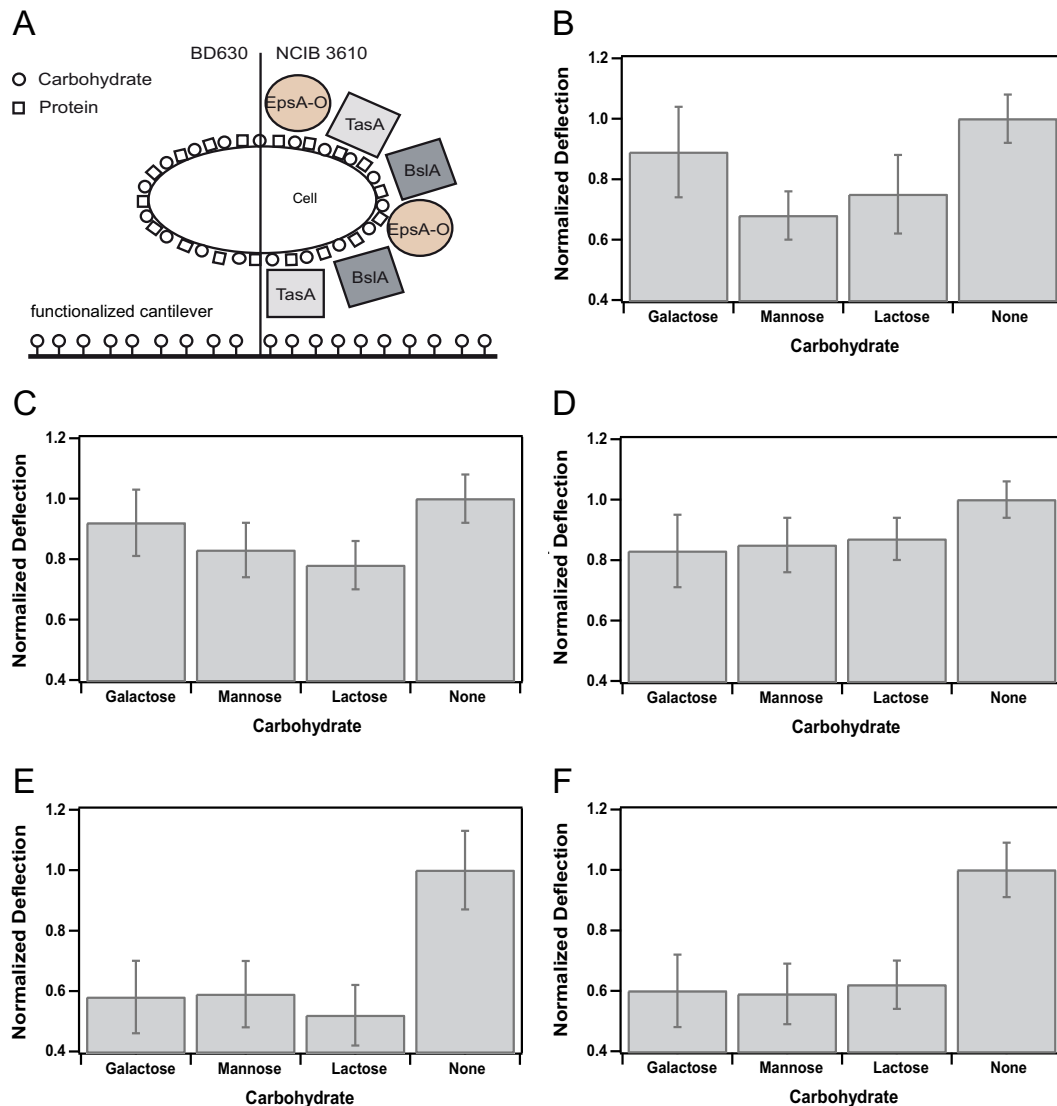
FIG 3 Attachment profile for *B. subtilis* strain NCIB 3610 and several mutant strains unable to express distinct biofilm matrix components. (A) Pictogram for the two *B. subtilis* wild-type strains used in the present study. Carbohydrates are depicted as circles, and proteins are depicted as squares. On the left, the wild-type strain BD630 that is unable to form a proper biofilm matrix is shown; on the right, the wild-type NCIB 3610 is depicted with the main components of its biofilm matrix. Please note that size and distribution of carbohydrates and proteins are not up to scale. (B to F) Attachment profiles (see Table S2 in the supplemental material) of all *B. subtilis* wild-type and mutant strains used in this study (Table 1) normalized to the values obtained for the unfunctionalized, pure gold cantilever (None). The average maximal deflection in dependence of the functionalization with a particular carbohydrate is depicted. Error bars indicate the standard deviations of the averaged and normalized maximal deflections. Attachment profiles for NCIB 3610 (B), TasA mutant (C), BslA mutant (D), EpsA-O mutant (E), and the wild-type strain BD630 (F) are shown.

ative of *B. subtilis* 168 that has the same ancestor as NCIB 3610, the so-called Marburg strain (46). *B. subtilis* 168 is not able to produce a proper biofilm matrix compared to NCIB 3610 due to several mutations and the lack of a plasmid required for biofilm formation (46). Since this strain lacks a proper biofilm matrix, especially the exopolysaccharide produced by the *epsA-O* operon, it can serve as a negative control. We find that similar to the EpsA-O knockout mutant, the reduction of bacterial adhesion to carbohydrate-coated gold cantilevers compared to the pure gold cantilevers was 40% (Fig. 3F). This finding supports our hypothesis that binding of *B. subtilis* NCIB 3610 to carbohydrate-coated cantilevers is facilitated by carbohydrate-carbohydrate interactions between the carbohydrates on the cantilever surface and the ex-

opolysaccharide produced by this biofilm-forming bacterium. The remaining 60% binding efficiency can be attributed to carbohydrate-carbohydrate or carbohydrate-protein interactions mediated by carbohydrates or proteins on the bacterial cell membrane.

DISCUSSION

We presented here a new approach for investigating bacterial adherence to different surfaces in real-time using the cantilever array technique. Focusing on the attachment of biofilm-forming bacteria, we found a strong adherence to gold cantilevers that might be explained by thiol-gold interactions (34) between the thiol groups of proteins present in the bacterial cell membrane or the biofilm

matrix proteins expressed at low levels in the stationary phase and the gold surface on the single cantilevers. Interestingly, adherence to gold cantilevers was most pronounced in a mutant and wild-type strain unable to produce an exopolysaccharide being part of the biofilm matrix (37, 45). This indicated that attachment of the biofilm-forming bacterium *B. subtilis* NCIB 3610 to gold surfaces was reduced by carbohydrates produced and secreted by this strain. To investigate whether carbohydrates are indeed able to reduce bacterial adhesion to gold surfaces, we coated our gold cantilevers with mono- and disaccharides and found that adhesion of *B. subtilis* NCIB 3610 to these carbohydrate-coated gold cantilevers was clearly reduced (Fig. 3), independent of the carbohydrate studied. The ability of carbohydrates to reduce bacterial adhesion to hydrophobic surfaces has been previously shown for complex glycoproteins such as mucin (6). Mucin is thereby thought to bind via a peptide backbone to hydrophobic surfaces, whereas hydrophilic oligosaccharide clusters stick out (6, 47). Our approach, reducing bacterial adhesion by coating of gold surfaces with mono- or disaccharides, has similar properties. First, our carbohydrates are bound via thiol groups to the hydrophobic gold surface and, second, mono- and disaccharides are exposed and able to interact with the bacterium. As described for mucin, we observed a reduction in bacterial adhesion when we coated our gold cantilevers with these carbohydrates, demonstrating that even mono- and disaccharide coating of hydrophobic surfaces can lead to a considerable reduction of bacterial adherence. Therein lies one important advantage of our approach since the extraction and purification of complex glycoproteins is no longer necessary. The technical approach presented here can be seen as a simple model system to study the reduction of bacterial adherence. Furthermore, the possibility to analyze bacterial adhesion to several surfaces in parallel, while studying different bacterial strains, allows for investigations of interactions mediating the bacterial adhesion. Carbohydrate-protein interactions are present in a wide range of biological relevant processes, such as bacterial infection or cell adhesion (48–50). One biologically important carbohydrate-protein interaction is the specific binding of carbohydrates to transport proteins in the bacterial cell membrane. After analyzing our different wild-type and mutant strains, we cannot attribute their adhesion to carbohydrate-coated gold cantilevers to specific interactions with carbohydrate transport or uptake systems, since *B. subtilis* does not possess transport systems for galactose or lactose (51, 52). It does possess a transport system for mannose (53), but since the binding strength to mannose-coated cantilevers is not significantly increased compared to the other two carbohydrates, we can exclude specific carbohydrate-transport system interactions as a major cause for adherence of the studied wild-type strain to our carbohydrate-coated cantilevers. We rather attribute the general bacterial adherence of this strain to unspecific interactions between carbohydrates or proteins in the bacterial cell wall and the carbohydrates on the cantilever surface. A mutant strain and a wild-type strain unable to produce one biofilm matrix component, namely, the exopolysaccharide (37, 45), were significantly reduced in their adherence to carbohydrate-coated gold cantilevers. This observation indicated that carbohydrate-carbohydrate interactions may facilitate the initial attachment of the biofilm-forming strain *B. subtilis* NCIB 3610, in this case by the interaction of the exopolysaccharide consisting of *N*-acetylgalactose, glucose, and galactose (36) and the carbohydrates on the cantilever surface. Carbohydrate-carbohydrate interactions were found to contribute to adhesion and recognition of eukaryotic cells (41, 43, 44), and adhesion forces with up to 300 piconewtons (38, 39) were detected. For bacteria, evidence for the existence of biologically significant carbohydrate-carbohydrate interactions is lacking. Still, bacteria could use carbohydrate interactions for the initial attachment to carbohydrate-coated surfaces. Understanding the underlying molecular interactions mediating bacterial adhesion will allow us to prevent bacterial infections in the future by suppressing bacterial attachment in the first place.

ACKNOWLEDGMENTS

REFERENCES

1. **Sauer K, Rickard AH, Davies DG.** 2007. Biofilms and biocomplexity. Microbe **2:**347–353.
2. **Donlan RM.** 2002. Biofilms: microbial life on surfaces. Emerg. Infect. Dis. **8:**881–890. http://dx.doi.org/10.3201/eid0809.020063.
3. **Flemming H, Griegbe W, Mayer C.** 2000. Physico-chemical properties of biofilms, p 19–34. *In* Evans LV (ed), Biofilms: recent advances in their study and control. Harwood Academic Publishers, Amsterdam, Netherlands.
4. **Coetser SE, Cloete TE.** 2005. Biofouling and biocorrosion in industrial water systems. Crit. Rev. Microbiol. **31:**213–232. http://dx.doi.org/10.1080/10408410500304074.
5. **Carpentier B, Cerf O.** 1993. Biofilms and their consequences, with particular reference to hygiene in the food industry. J. Appl. Bacteriol. **75:**499–511. http://dx.doi.org/10.1111/j.1365-2672.1993.tb01587.x.
6. **Shi L, Ardehali R, Caldwell KD, Valint P.** 2000. Mucin coating on polymeric material surfaces to suppress bacterial adhesion. Colloids Surf. B Biointerfaces **17:**229–239. http://dx.doi.org/10.1016/S0927-7765(99)00121-6.
7. **Klemm P, Vejborg R, Hancock V.** 2010. Prevention of bacterial adhesion. Appl. Microbiol. Biotechnol. **88:**451–459. http://dx.doi.org/10.1007/s00253-010-2805-y.
8. **Rachmaninov O, Zinger-Yosovich KD, Gilboa-Garber N.** 2012. Preventing *Pseudomonas aeruginosa* and *Chromobacterium violaceum* infections by anti-adhesion-active components of edible seeds. Nutr. J. **11:**10. http://dx.doi.org/10.1186/1475-2891-11-10.
9. **Ricciuto J, Heimer SR, Gilmore MS, Argüeso P.** 2008. Cell surface O-glycans limit *Staphylococcus aureus* adherence to corneal epithelial cells. Infect. Immun. **76:**5215–5220. http://dx.doi.org/10.1128/IAI.00708-08.
10. **O'Toole G, Kaplan HB, Kolter R.** 2000. Biofilm formation as microbial development. Annu. Rev. Microbiol. **54:**49–79. http://dx.doi.org/10.1146/annurev.micro.54.1.49.
11. **Kearns DB, Chu F, Branda SS, Kolter R, Losick R.** 2005. A master regulator for biofilm formation by *Bacillus subtilis*. Mol. Microbiol. **55:**739–749.
12. **Romero D, Aguilar C, Losick R, Kolter R.** 2010. Amyloid fibers provide structural integrity to *Bacillus subtilis* biofilms. Proc. Natl. Acad. Sci. U. S. A. **107:**2230–2234. http://dx.doi.org/10.1073/pnas.0910560107.
13. **Kobayashi K, Iwano M.** 2012. BslA(YuaB) forms a hydrophobic layer on the surface of *Bacillus subtilis* biofilms. Mol. Microbiol. **85:**51–66. http://dx.doi.org/10.1111/j.1365-2958.2012.08094.x.
14. **Hobley L, Ostrowski A, Rao FV, Bromley KM, Porter M, Prescott AR, MacPhee CE, van Aalten DM, Stanley-Wall NR.** 2013. BslA is a self-assembling bacterial hydrophobin that coats the *Bacillus subtilis* biofilm. Proc. Natl. Acad. Sci. U. S. A. **110:**13600–13605. http://dx.doi.org/10.1073/pnas.1306390110.
15. **Blair KM, Turner L, Winkelman JT, Berg HC, Kearns DB.** 2008. A molecular clutch disables flagella in the *Bacillus subtilis* biofilm. Science **320:**1636–1638. http://dx.doi.org/10.1126/science.1157877.

16. **Seminara A, Angelini TE, Wilking JN, Vlamakis H, Ebrahim S, Kolter R, Weitz DA, Brenner MP.** 2012. Osmotic spreading of *Bacillus subtilis* biofilms driven by an extracellular matrix. Proc. Natl. Acad. Sci. U. S. A. **109:**1116–1121. http://dx.doi.org/10.1073/pnas.1109261108.

17. **Wilking JN, Zaburdaev V, De Volder M, Losick R, Brenner MP, Weitz DA.** 2013. Liquid transport facilitated by channels in *Bacillus subtilis* biofilms. Proc. Natl. Acad. Sci. U. S. A. **110:**848–852. http://dx.doi.org/10.1073/pnas.1216376110.

18. **Vlamakis H, Aguilar C, Losick R, Kolter R.** 2008. Control of cell fate by the formation of an architecturally complex bacterial community. Genes Dev. **22:**945–953. http://dx.doi.org/10.1101/gad.1645008.

19. **Berk V, Fong JC, Dempsey GT, Develioglu ON, Zhuang X, Liphardt J, Yildiz FH, Chu S.** 2012. Molecular architecture and assembly principles of *Vibrio cholerae* biofilms. Science **337:**236–239. http://dx.doi.org/10.1126/science.1222981.

20. **Cogan NG, Donahue MR, Whidden M, De La Fuente L.** 2013. Pattern formation exhibited by biofilm formation within microfluidic chambers. Biophys. J. **104:**1867–1874. http://dx.doi.org/10.1016/j.bpj.2013.03.037.

21. **Fritz J.** 2008. Cantilever biosensors. Analyst **133:**855–863. http://dx.doi.org/10.1039/b718174d.

22. **Gruber K, Horlacher T, Castelli R, Mader A, Seeberger PH, Hermann BA.** 2011. Cantilever array sensors detect specific carbohydrate-protein interactions with picomolar sensitivity. ACS Nano. **5:**3670–3678. http://dx.doi.org/10.1021/nn103626q.

23. **Tzeng T-RJ, Saeidpourazar R, Aphale SS, Jalili N, Cheng YR.** 2010. Adhesin-specific nanomechanical cantilever biosensors for detection of microorganisms. J. Heat Transfer **133.** http://dx.doi.org/10.1115/1.4002363.

24. **Mader A, Gruber K, Castelli R, Hermann BA, Seeberger PH, Radler JO, Leisner M.** 2012. Discrimination of *Escherichia coli* strains using glycan cantilever array sensors. Nano Lett. **12:**420–423. http://dx.doi.org/10.1021/nl203736u.

25. **Maloney N, Lukacs G, Ball SL, Hegner M.** 2014. Device for filamentous fungi growth monitoring using the multimodal frequency response of cantilevers. Rev. Sci. Instrum. **85:**015003. http://dx.doi.org/10.1063/1.4854655.

26. **Nowicka AM, Hasse U, Sievers G, Donten M, Stojek Z, Fletcher S, Scholz F.** 2010. Selective knockout of gold active sites. Angewandte Chemie Int. Ed. **49:**3006–3009. http://dx.doi.org/10.1002/anie.201000485.

27. **Weissmüller J, Duan H.** 2008. Cantilever bending with rough surfaces. Phys. Rev. Lett. **101:**146102. http://dx.doi.org/10.1103/PhysRevLett.101.146102.

28. **Ratner DM, Plante OJ, Seeberger PH.** 2002. A linear synthesis of branched high-mannose oligosaccharides from the HIV-1 viral surface envelope glycoprotein gp120. Eur. J. Org. Chem. **2002:**826–833. http://dx.doi.org/10.1002/1099-0690(200203)2002:5<826::AID-EJOC826>3.0.CO;2-2.

29. **McKendry R, Zhang J, Arntz Y, Strunz T, Hegner M, Lang HP, Baller MK, Certa U, Meyer E, Guntherodt HJ, Gerber C.** 2002. Multiple label-free biodetection and quantitative DNA-binding assays on a nanomechanical cantilever array. Proc. Natl. Acad. Sci. U. S. A. **99:**9783–9788. http://dx.doi.org/10.1073/pnas.152330199.

30. **Giljohann DA, Seferos DS, Daniel WL, Massich MD, Patel PC, Mirkin CA.** 2010. Gold nanoparticles for biology and medicine. Angewandte Chemie Int. Ed. **49:**3280–3294. http://dx.doi.org/10.1002/anie.200904359.

31. **Van Houdt R, Michiels CW.** 2010. Biofilm formation and the food industry, a focus on the bacterial outer surface. J. Appl. Microbiol. **109:**1117–1131. http://dx.doi.org/10.1111/j.1365-2672.2010.04756.x.

32. **Wingender J, Flemming H-C.** 2011. Biofilms in drinking water and their role as reservoir for pathogens. Int. J. Hyg. Environ. Health **214:**417–423. http://dx.doi.org/10.1016/j.ijheh.2011.05.009.

33. **El-Taib HF, Shehata, Tantawy NS.** 2014. Integrity of metallic medical implants in physiological solutions. Int. J. Electrochem. Sci. **9:**18. http://www.electrochemsci.org/papers/vol9/90401986.pdf.

34. **Love JC, Estroff LA, Kriebel JK, Nuzzo RG, Whitesides GM.** 2005. Self-assembled monolayers of thiolates on metals as a form of nanotechnology. Chem. Rev. **105:**1103–1170. http://dx.doi.org/10.1021/cr0300789.

35. **Nuzzo RG, Allara DL.** 1983. Adsorption of bifunctional organic disulfides on gold surfaces. J. Am. Chem. Soc. **105:**4481–4483. http://dx.doi.org/10.1021/ja00351a063.

36. **Chai Y, Beauregard PB, Vlamakis H, Losick R, Kolter R.** 2012. Galactose metabolism plays a crucial role in biofilm formation by *Bacillus subtilis*. mBio **3:**e00184-12. http://dx.doi.org/10.1128/mBio.00184-12.

37. **Branda SS, Chu F, Kearns DB, Losick R, Kolter R.** 2006. A major protein component of the *Bacillus subtilis* biofilm matrix. Mol. Microbiol. **59:**1229–1238. http://dx.doi.org/10.1111/j.1365-2958.2005.05020.x.

38. **Bucior I, Scheuring S, Engel A, Burger MM.** 2004. Carbohydrate-carbohydrate interaction provides adhesion force and specificity for cellular recognition. J. Cell Biol. **165:**529–537. http://dx.doi.org/10.1083/jcb.200309005.

39. **Bucior I, Burger M.** 2004. Carbohydrate-carbohydrate interaction as a major force initiating cell-cell recognition. Glycoconj. J. **21:**111–123. http://dx.doi.org/10.1023/B:GLYC.0000044843.72595.7d.

40. **Ferrara C, Grau S, Jäger Sondermann CP, Brünker P, Waldhauer I, Hennig M, Ruf A, Rufer AC, Stihle M, Umaña P, Benz J.** 2011. Unique carbohydrate–carbohydrate interactions are required for high affinity binding between FcγRIII and antibodies lacking core fucose. Proc. Natl. Acad. Sci. U. S. A. **108:**12669–12674. http://dx.doi.org/10.1073/pnas.1108455108.

41. **Lorenz B, Álvarez de Cienfuegos L, Oelkers M, Kriemen E, Brand C, Stephan M, Sunnick E, Yüksel D, Kalsani V, Kumar K, Werz DB, Janshoff A.** 2012. Model system for cell adhesion mediated by weak carbohydrate-carbohydrate interactions. J. Am. Chem. Soc. **134:**3326–3329. http://dx.doi.org/10.1021/ja210304j.

42. **Santacroce PV, Basu A.** 2003. Probing specificity in carbohydrate-carbohydrate interactions with micelles and Langmuir monolayers. Angewandte Chemie Int. Ed. **42:**95–98. http://dx.doi.org/10.1002/anie.200390063.

43. **Hakomori S.** 1991. Carbohydrate-carbohydrate interaction as an initial step in cell recognition. Pure Appl. Chem. **63:**473–482.

44. **de la Fuente JM, Penades S.** 2004. Understanding carbohydrate-carbohydrate interactions by means of glyconanotechnology. Glycoconj. J. **21:**149–163. http://dx.doi.org/10.1023/B:GLYC.0000044846.80014.cb.

45. **Albano M, Hahn J, Dubnau D.** 1987. Expression of competence genes in *Bacillus subtilis*. J. Bacteriol. **169:**3110–3117.

46. **McLoon AL, Guttenplan SB, Kearns DB, Kolter R, Losick R.** 2011. Tracing the domestication of a biofilm-forming bacterium. J. Bacteriol. **193:**2027–2034. http://dx.doi.org/10.1128/JB.01542-10.

47. **Bansil R, Turner BS.** 2006. Mucin structure, aggregation, physiological functions, and biomedical applications. Curr. Opin. Colloid Interface Sci. **11:**164–170. http://dx.doi.org/10.1016/j.cocis.2005.11.001.

48. **Dwek RA.** 1996. Glycobiology: toward understanding the function of sugars. Chem. Rev. **96:**683–720. http://dx.doi.org/10.1021/cr940283b.

49. **Haltiwanger RS, Lowe JB.** 2004. Role of glycosylation in development. Annu. Rev. Biochem. **73:**491–537. http://dx.doi.org/10.1146/annurev.biochem.73.011303.074043.

50. **Ratner DM, Adams EW, Disney MD, Seeberger PH.** 2004. Tools for glycomics: mapping interactions of carbohydrates in biological systems. Chembiochem **5:**1375–1383. http://dx.doi.org/10.1002/cbic.200400106.

51. **Krispin O, Allmansberger R.** 1998. The *Bacillus subtilis* AraE protein displays a broad substrate specificity for several different sugars. J. Bacteriol. **180:**3250–3252.

52. **Krispin O, Allmansberger R.** 1998. The *Bacillus subtilis* galE gene is essential in the presence of glucose and galactose. J. Bacteriol. **180:**2265–2270.

53. **Sun T, Altenbuchner J.** 2010. Characterization of a mannose utilization system in *Bacillus subtilis*. J. Bacteriol. **192:**2128–2139. http://dx.doi.org/10.1128/JB.01673-09.

54. **Branda SS, González-Pastor JE, Ben-Yehuda S, Losick R, Kolter R.** 2001. Fruiting body formation by *Bacillus subtilis*. Proc. Natl. Acad. Sci. U. S. A. **98:**11621–11626. http://dx.doi.org/10.1073/pnas.191384198.